www.rericjournal.ait.ac.th

Hydrothermal Carbonization of Oil Palm Pressed Fiber: Effect of Reaction Parameters on Product Characteristics

Kamonwat Nakason*,+, Bunyarit Panyapinyopol*,+, Vorapot Kanokkantapong#,1, Nawin Viriya-empikul^, Wasawat Kraithong**, and Prasert Pavasant++

Abstract – *This work focused on the hydrothermal carbonization (HTC) of oil palm pressed fiber for the production of valuable products, over the reaction temperature (140 to 200 °C), time (1 to 4 h), and biomass to water content (BTW) (1:5 to 1:15). Reaction temperature was a vital key parameter on fuel properties of hydrochar. The combustibility of hydrochar reflected by fuel ratio increased from 0.42 at 140 °C to 0.54 at 200 °C. O/C and H/C atomic ratio decreased from 0.56 and 1.54 to 0.37 and 1.28, respectively, which corresponded to an increase in the estimated HHV from 21.0 to 24.6 MJ/kg. Hydrochar yield decreased from 78.4 to 61.7%. These phenomena were associated with hydrolysis, dehydration, decarboxylation, aromatization, and recondensation reactions. The reaction time and BTW affected slightly the yield and fuel properties of hydrochar. The valuable dissolved organic chemical species in the obtained liquid fraction were furfuryl alcohol, furfural, hydroxymethylfurfural, acetic acid, propionic acid, lactic acid, and formic acid with the maximum yields of 6.95, 2.05, 0.64, 6.91, 4.75, 4.11 and 2.64 wt.% dry raw material, respectively.*

Keywords – biofuels, biomass, hydrochar, intermediate chemicals, lignocellulosic materials.

1. INTRODUCTION

Hydrothermal carbonization (HTC) is a high potential technology in the field of biomass utilization due to its several advantages. HTC can be conducted at 150 to 250°C which was lower than other thermochemical conversion technologies, e.g. combustion, pyrolysis, and gasification [1]. During HTC, biomass is converted in hot compressed water, excluding the energy intensive pre-drying step [2]. The products from HTC include hydrochar, liquid fraction, and gases, obtained under the networks of hydrolysis, dehydration, decarboxylation, aromatization, and recondensation reactions [3]. Hydrochar is the major product with high carbon content, grindability, and hydrophobicity properties. Liquid fraction is considered as a by-product stream containing many valuable organic chemicals such as furfural, hydroxymethylfurfural, lactic acid, formic acid, acetic acid, and levulinic acid [5-7].

Recent literature demonstrates the possibility of converting several types of biomass to hydrochar, such as oil palm empty fruit brunch [8], corn stalk [9], olive stone [10], waste eucalyptus bark [11], and poplar wood [12]. However, hydrochar characteristics were substantially different based on the type of feedstocks and process variables such as process temperature, residence time, and biomass to water (BTW) content [13-15].

Oil palm is one of the economic crops in Thailand. In 2015, oil palm production was about 11 million tons and this increased continuously from previous years [16]. Recently, the upgrading of oil palm shell [17], oil palm trunk and fronds [18], and oil palm empty fruit bunch [5, 8] by HTC were performed. However, the HTC of oil palm pressed fiber (OPPF) has been restricted, and liquid fraction characteristics from HTC of oil palm residues has not been revealed. OPPF is waste generated from oil palm industry where the residue product ratio is approximately 0.19 tons/ton oil palm product [19]. Thus, the amount of OPPF was about 2.09 million tons in 2015. In order to add value to OPPF and summarize the liquid fraction characteristics from HTC, the upgrading of OPPF under high potential technology must be conducted.

Indeed, the purposes of this study are to; (1) investigate the properties of hydrochar and liquid fraction obtained from HTC of OPPF, and (2) examine the effect of operating parameters including temperature, residence time, and BTW content on HTC product characteristics.

2. MATERIALS AND METHODS

2.1 Feedstock

Oil palm pressed fiber (OPPF) was used as a substrate in this study. It was collected from Suksomboon Palm Oil Co., Ltd., Chonburi Province, Thailand. To stock the material, OPPF was dried at 70°C for 24 h and milled to

*Department of Sanitary Engineering, Faculty of Public Health, Mahidol University, Bangkok, Thailand.

+Center of Excellence on Environmental Health and Toxicology (EHT), Bangkok, Thailand.

#Department of Environmental Science, Faculty of Science, Chulalongkorn University, Bangkok, Thailand.

^The Joint Graduate School of Energy and Environment, King Mongkut's University of Technology Thonburi, Bangkok, Thailand.

**National Nanotechnology Center (NANOTEC), National Science and Technology Development Agency (NSTDA), Pathumthani, Thailand.

++Department of Chemical Engineering, School of Energy Science and Engineering, Vidyasirimedhi Institute of Science and Technology, Rayong, Thailand

1 Corresponding author;
Tel: +662 2185 186.
E-mail: vorapot.ka@chula.ac.th

the particle size of less than 0.1 mm. After that, OPPF powder was dried at 105 °C for 12 h and stored in a sealed plastic bag. Table 1 shows the original properties of OPPF.

Table 1. Properties of OPPF (%wt. on dry basis).

Characteristics		Content
Proximate analysis	Moisture	32.2
	Ash	5.9
	VM	67.3
	FC	26.8
Ultimate analysis	C	48.2
	H	6.1
	N	1.3
	S	0.2
	O	38.3
HHV (MJ/kg)		20.0

2.2 Hydrothermal Carbonization (HTC) Process

HTC of OPPF was performed in a batch bomb stainless steel reactor (500 ml, NK Laboratory Co., Ltd, Thailand). 70, 38, and 25 g OPPF powder mixed with 345, 377, and 390 ml of deionized water, respectively, was filled in the fitting glass liner (equal to 1:5, 1:10, and 1:15 biomass to water content or BTW). The working volume used in this study was 400 ml. The reactor was tightly sealed and heated to the desired temperature (140, 160, 180 and 200 °C) with the heating rate of 1 °C/min for 3 h. The desired temperature was measured in the mixture of biomass and water by a pipe-fitting thermocouple probe (Type K). During the experiment with varying reaction times at 1, 2, 3, and 4 h, the process condition was set at 200 °C and 1:10 of BTW. After the reaction completed, the reactor was submerged in the ice-water bath to cool down to the ambient temperature rapidly. Hydrochar was separated from the liquid fraction by vacuum filtration, and it was washed with deionized water until the pH of washed water was neutral. After that it was dried at 105 °C overnight. The dried hydrochar was stored in a sealed plastic bag for further analysis. All experiments were conducted in duplication.

2.3 Analysis of Products Characteristic

2.3.1 Hydrochar Analysis

Ultimate analysis of OPPF and hydrochar was performed using an elemental analyzer (LECO CHNS 628, LECO, USA). The contents of ash and volatile matter (VM) were measured according to the method of NREL/TP-510-42622 [20] and ASTM D 7582 [21], respectively. Fixed carbon (FC) content was identified by deducting 100% from ash and VM contents. Functional groups of hydrochar were determined by fourier transform infrared spectroscopy (FTIR) (Thermo Scientific Nicolet 6700, Thermo Scientific, USA). Thermal decomposition behavior of OPPF and hydrochar was observed with a thermogravimetric analyzer (TGA) (TGA/SDTA851e, METTLER TOLEDO, USA). The analysis was performed between the temperature range of 25-900 °C at a heating rate of 10 °C/min under nitrogen atmosphere with the flow rate of 20 ml/min.

2.3.2 Characterization of Liquid Fraction

After quenching of reaction, pH level was measured immediately (Series Meters - S20, METTLER TOLEDO, USA). Yield of valuable dissolved organic chemical species including furfural, furfuryl alcohol, hydroxylmethylfurfural (HMF), lactic acid, formic acid, acetic acid, levulinic acid, and propionic acid were determined through the concentration of each substance using the high performance liquid chromatography (HPLC) (Shimadzu 10A, Shimadzu, Japan). The HPLC instruments were installed with a Bio-Rad Organic Acid column Aminex HPX-87H and UV-Vis detectors (SPD-20A, Shimadzu, Japan), 0.6 cm^3/min of 5 mM sulfuric acid in water used as a mobile phase. The concentrations of each chemical in the sample were calculated using calibration curves obtained from the standard solution with accurately determined concentration.

2.3.3 Calculations

Hydrochar yield (HY), energy densification (ED), energy yield (EY), carbon densification (CD), carbon yield (CY), and fuel ratio are calculated from:

$$HY\ (\%) = (\text{mass of total dried hydrochar} / \text{mass of total dried feedstock}) \times 100\% \quad (1)$$

$$ED = \text{HHV of dried hydrochar} / \text{HHV of dried feedstock} \quad (2)$$

$$EY\ (\%) = HY \times ED \quad (3)$$

$$CD = \text{Carbon content of dried hydrochar} / \text{Carbon content of dried feedstock} \quad (4)$$

$$CY\ (\%) = HY \times CD \quad (5)$$

$$\text{Fuel ratio} = FC / VM \quad (6)$$

The HHV of hydrochar was estimated using Equation 7 proposed by [22]:

$$HHV\ (MJ \cdot kg^{-1}) = 0.3491C + 1.1783H + 0.1005S - 0.1034O - 0.0151N - 0.021A \quad (7)$$

where, C, H, O, N, S and A represent the mass percentages on dry basis of carbon, hydrogen, oxygen, nitrogen, sulfur and ash contents of samples, respectively. The HHV improvement can be defined as:

$$\text{HHV improvement} = (\text{HHV of hydrochar} - \text{HHV of feedstock}) / \text{HHV of feedstock} \quad (8)$$

Yields of furfural, furfuryl alcohol, HMF, lactic acid, formic acid, acetic acid, levulinic acid, and propionic acid are calculated from Equation 9:

$$Y_x = M_x/M \times 100\% \quad (9)$$

where, Y_x (x = 1, 2, 3, 4, 5, 6, 7, or 8) are yields of furfural, furfuryl alcohol, HMF, lactic acid, formic acid, acetic acid, levulinic acid, and propionic acid, respectively; M_x are masses of furfural, furfuryl alcohol,

HMF, lactic acid, formic acid, acetic acid, levulinic acid, and propionic acid, respectively; and M is the total mass of dry biomass.

3. RESULTS AND DISCUSSION

3.1 Hydrochar Characterization

3.1.1 Hydrochar Yield

Hydrochar yield obtained from hydrothermal carbonization (HTC) of oil palm pressed fiber (OPPF) at different reaction temperature, time and biomass to water content (BTW) is summarized in Figure 1. As a function of reaction temperature, hydrochar yield decreased from 78.4% at 140 °C to 61.7% at 200 °C which may be due to the partial dissolving and hydrolyzation of biomass composition. The yield obtained in this study was in a similar range as that reported by Zakaria *et al.* [23]. They found that hydrochar yield of oil palm empty fruit bunch decreased from 67.8 to 52.7% by increasing reaction temperature from 210 to 250 °C at 20 min. Studies of reaction time variation on hydrochar yield was performed at temperature of 200 °C and BTW of 1:10 with different reaction times. By increasing reaction time from 1 to 4 h, hydrochar yield decreased marginally from 62.9 to 61.5% which was similar to the report of Rather *et al.* [24]. They revealed that an increase in reaction time from 10 to 40 min in HTC of macrophyte Potamogeton lucens, hydrochar yield decreased from 42 to 39%. The effect of BTW of 1:5, 1:10, and 1:15 was observed at reaction temperature of 200 °C for 3 h of reaction time. Hydrochar yield decreased slightly from 61.9% at 1:5 to 59.0% at 1:15. Similar results were revealed by Rather *et al.*, Singh *et al.*, and Anastasakis *et al.* [24]-[26], who performed HTC of macrophyte Potamogeton lucens, macroalgae Laminaria saccharina, and water hyacinth, respectively. As can be seen, reaction temperature had a higher impact on hydrochar yield than reaction time and BTW, and this agreed well with Gao *et al.* [11] and Rather *et al.* [24].

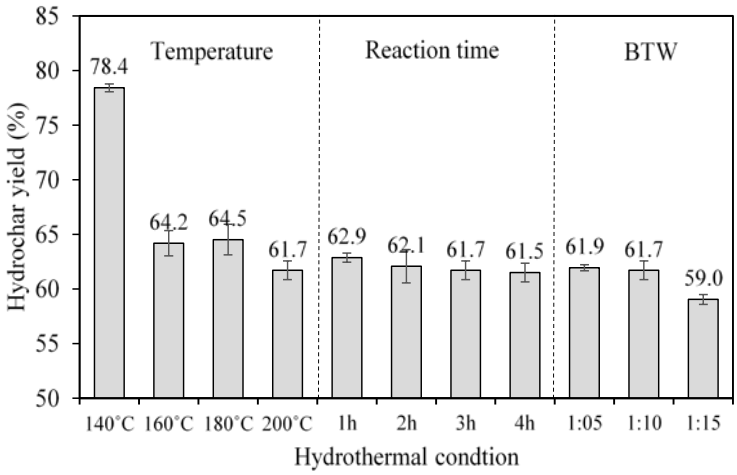

Fig. 1. Hydrochar yield obtained from OPPF by different reaction temperature (140, 160, 180, 200 °C for 3 h and BTW of 1:10), reaction time (1, 2, 3, 4 h at 200 °C and BTW of 1:10) and solid per liquid ratio (1:5, 1:10, 1:15 for 3 h and 200 °C).

3.1.2. Physicochemical Characteristics and Elemental Related Properties

The results of proximate and ultimate analysis of hydrochar obtained from HTC of OPPF are presented in Table 2. Proximate analysis showed that ash content decreased significantly from 5.90% of OPPF to 4.65% of hydrochar obtained at temperature 140 °C. This phenomenon may be due to the release of inorganic compositions from biomass into liquid fraction [27]. This, however, increased to 5.33% when the reaction temperature increased to 200 °C, and this was probably due to the re-absorption of inorganic components as reaction temperature increased, whereas some of inorganics may be deposited on hydrochar. Consistent results were reported by Kongpanya *et al.* [8] and Ahmad *et al.* [18] who converted oil palm empty fruit bunch, and oil palm frond and trunk, respectively. In the case of oil palm empty fruit bunch, ash content decreased from 14.18% of raw material to 1.76% of hydrochar obtained from HTC at 100 °C for 90 min. This ash then increased to 2.45% of hydrochar obtained from HTC at 200 °C for 90 min. It was noted that the change of reaction time and BTW was only reported to only slightly affect the ash content.

The volatile matter (VM) content was found to decrease as a function of reaction temperature from 67.0% at 140 °C to 60.4% at 200 °C in response to an increase in fixed carbon (FC) content from 28.4 to 34.2%. In addition, fuel ratio (FC/VM) used to evaluate the combustibility of hydrochar increased from 0.42 to 0.57 with an increase in reaction temperature from 140 to 200 °C. The effect of reaction time and BTW on VM content were negligible. Similar results were revealed by Ahmad *et al.* [18], who reported that VM content of hydrochar obtained from HTC of oil palm frond decreased from 79.5% at 200 °C to 45.2% at 350 °C for 0.5 h, whereas FC content increased from 20.5 to 54.8% and increased in fuel ratio from 0.26 to 1.21.

Table 2.Proximate and ultimate analysis of hydrochar obtained at various reaction temperature (140, 160, 180, 200 °C), time (1, 2, 3, 4 h), and biomass to water content (BTW) (1:5, 1:10, 1:15).

	Ultimate analysis (wt.%, dry basis)					Proximate analysis (wt.%, dry basis)			Estimated HHV (MJ/kg)	HHV improvement	Fuel ratio
	C	H	N	S	O	Ash	VM	FC			
Temperature (°C) (Time 3 h, BTW 1:10)											
140	50.0	6.42	1.24	0.17	37.7	4.65	67.0	28.4	21.0	0.05	0.42
160	53.5	6.35	1.31	0.21	33.7	4.94	64.7	30.3	22.6	0.13	0.47
180	56.5	6.19	1.23	0.16	30.9	5.10	62.0	33.0	23.7	0.19	0.53
200	58.2	6.23	1.27	0.16	28.8	5.33	61.3	33.4	24.6	0.23	0.54
Time (h) (Temperature 200°C, BTW 1:10)											
1	55.9	6.22	1.22	0.17	31.1	5.34	61.7	32.9	23.5	0.18	0.53
2	57.2	6.17	1.19	0.18	30.1	5.20	60.8	34.0	24.0	0.20	0.56
3	58.2	6.23	1.27	0.16	28.8	5.33	61.3	33.4	24.6	0.23	0.54
4	58.8	6.18	1.30	0.17	28.1	5.42	60.4	34.2	24.8	0.24	0.57
BTW (Temperature 200°C, Time 3h)											
1:5	57.3	5.95	1.27	0.17	30.0	5.35	61.7	32.9	23.8	0.19	0.53
1:10	58.2	6.23	1.27	0.16	28.8	5.33	61.3	33.4	24.6	0.23	0.54
1:15	56.3	6.00	1.23	0.15	30.8	5.49	60.5	34.0	23.4	0.17	0.56

Ultimate analysis results illustrate that, by increasing reaction temperature from 140 to 200 °C, carbon content rose from 50.0 to 58.2%, whereas oxygen content reduced from 37.7 to 28.8%, and hydrogen content decreased from 6.4 to 6.2%. In comparison with increasing of reaction time from 1 to 4 h, carbon content increased from 55.9 to 58.8%, oxygen content decreased from 31.1 to 28.1%, and hydrogen content was nearly constant. The influence of BTW on ultimate analysis results was negligible. Since the estimated HHV relied on elemental compositions, an increase in reaction temperature from 140 to 200 °C led to an increase in estimated HHV from 21.0 to 24.6 MJ/kg. An increase in reaction time from 1 to 4 h was associated with an increase in estimated HHV from 23.5 to 24.8 MJ/kg. Again, the effect of BTW on estimated HHV was negligible. In terms of HHV improvement (compared with the raw material), raising reaction temperature from 140 to 200 °C resulted in an increase in HHV improvement from 0.05 to 0.23, whereas, an increase in reaction time from 1 to 4 h resulted in HHV improvement increasing from 0.18 to 0.24. Consistent results were reported by Ahmad *et al.* [18] where HHV of hydrochar obtained from HTC of oil palm trunk increased from 19.9 to 29.7 MJ/kg with increasing reaction temperature from 200 to 350 °C for 0.5h, which corresponded to an increase in HHV improvement from 0.06 to 0.58.

Van-Krevelen diagram is a useful way to describe the fuel properties of solid fuel through elemental content [28]. In this diagram, O/C and H/C atomic ratio of biomass and hydrochar were plotted. A better fuel property was located close to the origin and vice versa [29]. Raw OPPF was located on the upper right corner of Figure 2, and hydrochar moved closer to the origin. O/C and H/C atomic ratio of hydrochar decreased from 0.56 and 1.54 to 0.37 and 1.28, respectively, by increasing reaction temperature from 140 to 200 °C. An increase in reaction time from 1 to 4 h resulted in O/C and H/C atomic ratio of hydrochar decreasing from 0.42 and 1.33 to 0.36 and 1.26, respectively. Note that O/C and H/C atomic ratio were virtually unaltered by varying BTW. The findings in this work were similar to those from oil palm empty fruit bunch (OPEFB) [5], and oil palm frond (OPF) and trunk (OPT) [18]. O/C and H/C atomic ratio of hydrochar from OPEFB decreased from 0.62 to 0.37 and 1.39 to 1.02 with an increase in reaction temperature from 180 to 220 °C for 22 h of reaction time.

The influence of HTC on biomass was estimated by calculating the energy-related properties of hydrochar, including the carbon densification (CD), carbon yield (CY), energy densification (ED), and energy yield (EY) as illustrated in Figure 3. To determine the densification of carbon in the hydrochar, CD was calculated (dry basis) where an increase in reaction temperature from 140 to 200 °C increased CD of hydrochar from 1.05 to 1.22. Increasing reaction time from 1 to 4 h led to a slight increase in CD from 1.18 to 1.24. In this case, the effect of BTW on CD was ignored. Consistent results were reported by Ahmad *et al.* [18], where CD of hydrochar obtained from HTC of oil palm frond and trunk increased from 1.14 to 1.59 and 1.08 to 1.59, respectively, with an increase in reaction temperature from 200 to 350 °C at 0.5 h of reaction time. CY is used to investigate the fraction of feedstock carbon retained within the hydrochar (based on dry basis). In this study, the highest CY of hydrochar was 82.42% obtained at 140 °C for 3 h.

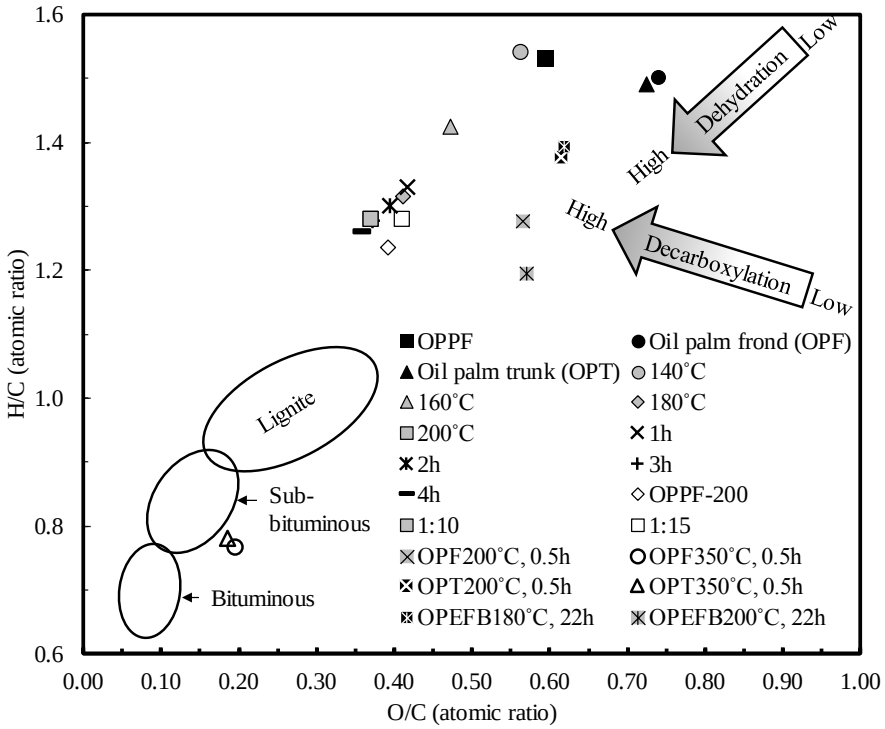

Fig. 2. Van-Krevelen diagram of OPF, hydrochars from different reaction temperatures, times, BTW content, and fuel coals including lignite [30], sub-bituminous, and bituminous [31].

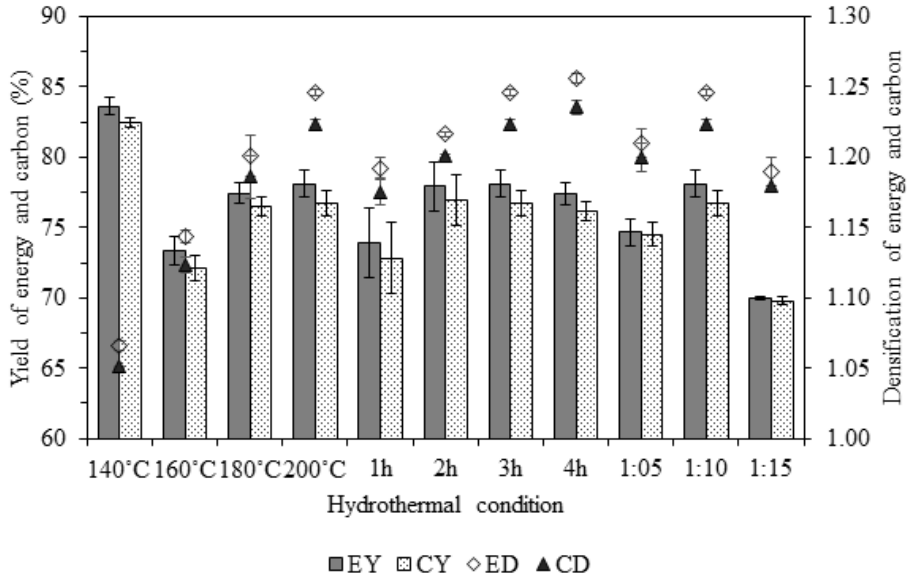

Fig. 3. ED, EY, CD, CY of hydrochar of OPPF by different reaction temperature (140, 160, 180, 200 °C), reaction time (1, 2, 3, 4 h) and solid per liquid ratio (1:5, 1:10, 1:15).

ED is densification of solid energy content (based on dry basis) [32]. With an increase in reaction temperature from 140 to 200 °C, ED of hydrochar increased from 1.07 to 1.25. Similarly, an increase in reaction time from 1 to 4 h enhanced ED of hydrochar from 1.19 to 1.26. Again, BTW only had marginal effect on ED of hydrochar. Similar results were found in ED of hydrochar from oil palm frond (OPF) and trunk (OPT) [18], where an increase in ED from 1.09 to 1.58 and 1.06 to 1.58, respectively, could be obtained by increasing reaction temperature from 200 to 350 °C at 0.5 h of reaction time. In addition, as EY was used to determine the fraction of feedstock energy retained within the hydrochar, Figure 3 illustrates that EY of hydrochar was varied with the process condition, where the highest EY of hydrochar was 83.59% and this was obtained from HTC at 140 °C for 3 h.

3.1.3 Thermal Decomposition Behavior

Thermal decomposition behavior of OPPF and hydrochar obtained from different reaction temperature for 3 h and BTW of 1:10 are illustrated by TGA and DTG curves in Figure 4. Thermal decomposition characteristics of OPPF composed of three major stages.

The first stage appeared at a temperature ranging from 30 to 150 °C, with one sharp peak at 100 °C, due to the weight loss of moisture and some volatile organic content. As for hydrochar, thermal decomposition in this stage was in the temperature range from 50 to 105 °C which was less narrow than original biomass because some portion of organic component was already degraded during HTC. The second stage, weight loss in the temperature range of 200 to 375 °C with two sharp peaks presented at 280 and 360 °C, was ascribed to the decomposition of hemicellulose and cellulose [33], respectively. The thermal decomposition of hydrochar in this stage in the temperature range of 200 to 400 °C with only one sharp peak at 370 °C was identified, and the weight loss of hydrochar decreased continuously from 0.71 to 0.10%/min with an increase in reaction temperature from 140 to 200 °C. Similar results of thermal decomposition behavior of hydrochar were also found by several studies such as waste eucalyptus bark [11] and cellulose, hemicellulose, lignin [34]. The last stage was presented due to the decomposition of lignin in the temperature range from 410 – 600 °C, and this was due to the existence of aromatic ring with various branches. In addition, Figure 4 illustrates that the rate of weight loss of hydrochar synthesized at higher temperature was lower than that of hydrochar synthesized at lower temperature. The remaining solid after TGA at high HTC temperature was higher than that at low temperature implying that hydrochar synthesized at higher reaction temperature was thermally more stable than that synthesized at lower temperature.

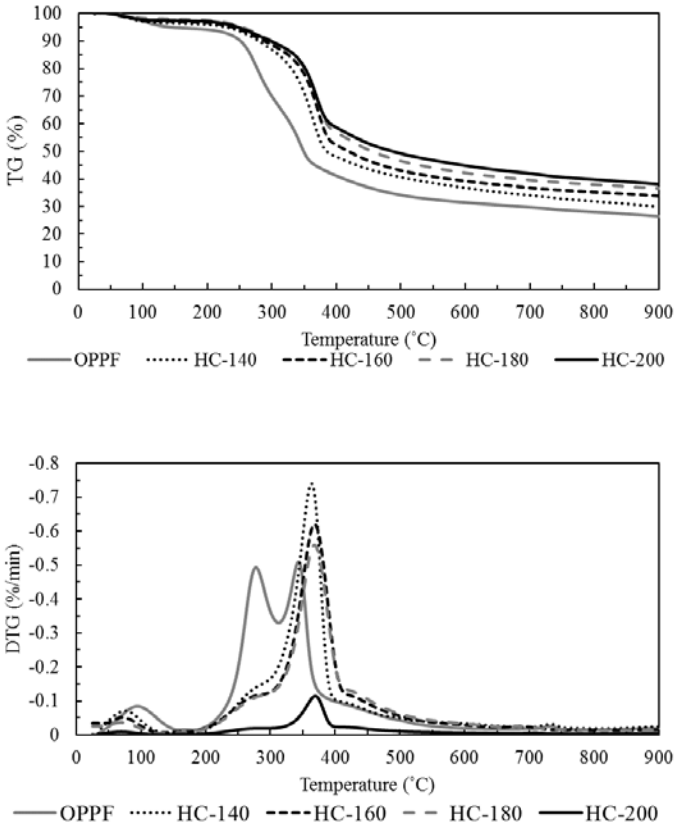

Fig. 4. Thermal decomposition behavior of OPPF and hydrochar by the reaction temperature of 140, 160, 180, and 200 °C for 4 h of reaction time.

3.1.4 FTIR Spectra

Figure 5 depicts FTIR spectra of OPPF and hydrochar obtained by different reaction temperature. The region peak presents at 3500-3300 cm^{-1} was attributed to O-H stretching vibration of hydroxyl. It became less intense with an increase in reaction temperature which corresponded with the dehydration reaction and related to the decrease in oxygen content. The transmittance peak at around 2900-2800 cm^{-1} were related to aliphatic C-H stretching vibration, and asymmetric and symmetric -C-H stretching of the methylene groups [35] where the peak of OPPF was of higher intensity than that of hydrochar. The present band at 1700 and 1600 cm^{-1} was due to C=C vibrations in aromatic ring structure [24]. The peak at 1157 cm^{-1} could be assigned to the C-O-C of glycosidic bonds of cellulose [36], and this peak of hydrochar was more intense than the feedstock due to the removal of amorphous components during HTC. The band at 1105 cm^{-1} was ascribed to the C-O stretching vibration of secondary alcohol, and that at 1025 cm^{-1} was assigned of C-OH from alcohol and/or alkyl substituted ethers groups.

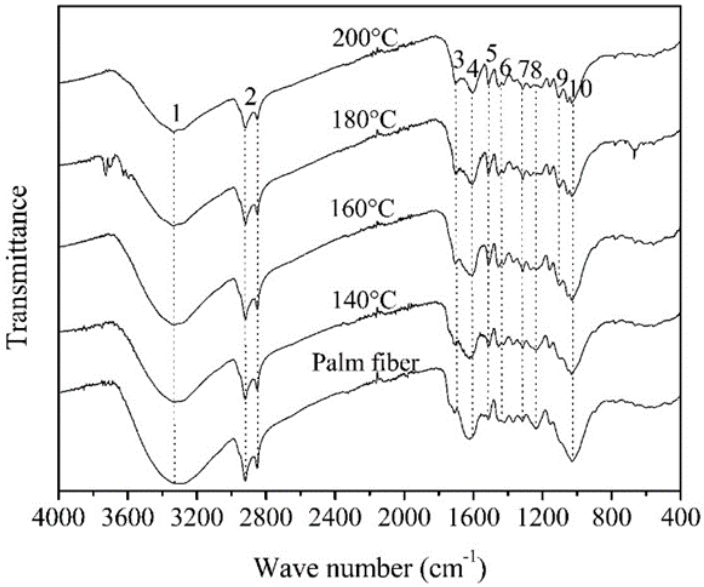

Fig. 5. FTIR spectra of OPPF and hydrochar produced at 140, 160, 180, and 200 °C for 4 h.

3.2 Liquid Fraction Characterization

Yield dissolved organic chemicals and pH level in liquid fraction (LF) by different reaction temperature (140, 160, 180, 200 °C for 3 h and biomass to water content (BTW) of 1:10), reaction time (1, 2, 3, 4 h at 200 °C and BTW of 1:10), and BTW (1:5, 1:10, 1:15 at 200 °C for 3 h) are illustrated in Table 3. In this study, pH level of LF decreased with increasing process temperature from 140 to 180 °C because of the further conversion of reducing sugar to organic acid. pH level raised with a further increase in reaction temperature to 200 °C. This may be due to aromatization and recondensation reactions of organic acids. The reaction time and BTW only marginally affected pH level. Valuable dissolved organic chemical species in LF by-product stream obtained from hydrothermal carbonization (HTC) of oil palm pressed fiber (OPPF) included furan compound (furfural, furfuryl alcohol, HMF) and low molecular organic acid (lactic acid, formic acid, acetic acid, levulinic acid, and propionic acid).

3.2.1 Furan Compound Yield

Based on the analysis result of LF, furfural was resulted from the dehydration reaction of xylose, and it is regarded as a value-added chemical if used as a precursor for resin, plastic and solvent [37]. In LF of OPPF, furfural yield increased with an increase in process temperature from 140 to 180 °C. An increase in retention time from 1 to 4 h saw a continual decrease in furfural yield. The change of BTW from 1:5 to 1:15 increased the furfural yield. Furfural could be further transformed to furfuryl alcohol, furan, and tetrahydrofuran [38] and this might be the reason for the decrease in furfural yield. In this study, the highest furfural yield of 2.05% was obtained at 180 °C for 3 h which agreed well to literature. Zakaria *et al.* [23] reported furfural yield of 3.74% obtained from hydrothermal pretreatment of oil palm frond fiber at 210 °C, 10 min.

Furfuryl alcohol is a result from the selective hydrogenation reaction of furfural [38], and it is considered as a valuable-added organic precursor for polymeric microspheres [39]. In this study, the yield of furfuryl alcohol was raised by raising the reaction temperature from 140 to 200 °C. On the other hand, it decreased with increasing of reaction time from 1 to 4 h at 200 °C. The decrease in furfuryl alcohol yield was probably related to a further hydrolysis to lactic acid [38], and lactic acid could be dehydrated to acrylic acid [40]. Changes of yield of furfuryl alcohol and lactic acid relied on reaction rate of selective hydrogenation, hydrolysis, and dehydration. The change of BTW from 1:5 to 1:15 was corresponded to an increase in furfuryl alcohol yield. In this study, the highest furfuryl alcohol yield of 6.95% was obtained at 200 °C for 1 h.

HMF was obtained from the dehydration reaction of hexose [41, 42], and it is useful because it can be used in the industries of chemical, polymer, resin, and solvent [43]. In this study, HMF yield increased while raising reaction temperature from 140 to 180 °C. On the other hand, the HMF yield decreased with increasing reaction time from 1 to 4 h. The change of BTW from 1:5 to 1:15 related to an increase in HMF yield. The highest HMF yield of 0.64% was obtained at 200 °C for 3 h and BTW of 1:15 which was lower than that from hydrothermal pretreatment of oil frond fiber at 210 °C for 10 min (1.84% HMF) [18].

3.2.2 Low Molecular Organic Acid Yield

The analysis of low molecular organic acid yield noted that, acetic acid, lactic acid, formic acid, and propionic acid were the basis organic acid compositions in LF obtained by HTC of OPPF. Acetic acid is very useful in anaerobic fermentation [7]. Its yield increased significantly by increasing of reaction temperature and time from 140 to 200 °C and 1 to 4 h. However, it was nearly constant by varying BTW. The maximum acetic acid yield in this study (6.91%) was obtained at 200 °C

for 3 h and BTW of 1:5 which was similar to acetic acid yield of oil palm frond fiber (7.17%) [18].

Formic acid is useful for hydrogen production [44], while lactic acid can be used as a precursor of biodegradable plastic polylactic acid, precursor of acrylic acid, metal pickling, and food additives [45, 46]. In this study, yields of these compounds increased with an increase in reaction temperature, time and BTW. The maximum yields of formic and lactic acids were 2.64 and 4.11%. Similar results were reported by Zakaria *et al.* [23] where formic acid yield of 4.82% was obtained from hydrothermal pretreatment of oil palm frond fiber at 210 °C for 10 min.

Propionic acid is a vital intermediate chemical in the synthesis of cellulose fibers, perfumes, herbicides, and pharmaceuticals [47]. In this study, the yield of propionic acid increased with an increase in reaction temperature and time from 140 to 180 °C and 1 to 4 h. In addition, the change of BTW from 1:5 to 1:15 increased the propionic yield with the maximum propionic yield of 4.75% obtained at 200 °C for 4 h and BTW of 1:10.

Table 3. pH level and yield of dissolved organic compositions in liquid fraction.

	pH	Furfural	Furfuryl alcohol	HMF	Lactic acid	Formic acid	Acetic acid	Levulinic acid	Propionic acid
Temperature (°C) (Time 3 h, BTW 1:10)									
140	4.30	0.13	0.00	0.08	0.00	0.26	1.76	0.00	0.10
160	3.85	1.10	1.36	0.07	0.68	0.00	3.76	0.15	2.29
180	3.70	2.05	3.04	0.63	2.64	0.97	5.29	0.93	3.76
200	3.88	0.44	3.09	0.33	2.57	4.11	6.74	3.74	4.52
Time (h) (Temperature 200 °C, BTW 1:10)									
1	3.75	1.63	6.95	0.51	0.00	0.79	0.00	0.79	0.00
2	3.84	0.57	3.50	0.38	0.36	1.04	0.00	0.86	0.09
3	3.88	0.44	3.09	0.33	2.57	4.11	6.74	3.74	4.52
4	3.80	0.55	2.23	0.14	1.86	1.39	6.89	2.33	4.75
BTW (Temperature 200 °C, Time 3 h)									
1:5	3.88	0.56	2.18	0.30	1.85	1.42	6.91	0.00	4.41
1:10	3.86	0.44	3.09	0.33	2.57	4.11	6.74	3.74	4.52
1:15	3.80	1.00	4.26	0.64	2.77	1.43	6.14	0.70	3.76

4. CONCLUSIONS

In the present study, oil palm pressed fiber (OPPF) was upgraded to hydrochar via hydrothermal carbonization (HTC) by changing reaction temperature from 140 to 200 °C, exposure time from 1 to 4 h, and biomass to water content (BTW) from 1:5 to 1:15. The results showed that reaction temperature is a vital key role on fuel properties of hydrochar. An increase in reaction temperature from 140 to 200 °C enhanced the biomass conversion which adversely affected hydrochar yield. The fuel ratio increased from 0.42 to 0.54. O/C and H/C atomic ratio decreased from 0.56 and 1.54 to 0.37 and 1.28, respectively, which was associated to an increase in HHV from 21.0 to 24.6 MJ/kg. In addition, a better thermal stability of hydrochar was presented at high reaction temperature. The reaction time and BTW only slightly affected the yield and fuel properties of hydrochar. Liquid fraction was regarded as by-product, and it contained high valuable dissolved organic chemicals including furfural, furfuryl alcohol, HMF, and low molecular organic acids which are valuable feedstocks for many industries. These findings indicated that OPPF could be mildly converted to solid biofuel and valuable dissolved organic chemicals via HTC. Future work should be directly towards the purification of such chemicals and how to viably scale up the system to commercial scale.

ACKNOWLEDGEMENTS

The research project was supported by Mahidol University, Nanomaterial for Energy and Catalyst Laboratory, National Nanotechnology Center (NANOTEC), National Science and Technology Development Agency (NSTDA) and the Sci Super III Fund (Ratchadaphiseksomphot Endowment). The study was supported for publication by the China Medical Board (CMB), Faculty of Public Health, Mahidol University, Bangkok, Thailand. Financial assistance for this research was also provided by the Center of Excellence on Environmental Health and Toxicology (EHT), Bangkok, Thailand.

REFERENCES

[1] Erdogan E., Atila B., Mumme J., Reza M.T., Toptas A., Elibol M., and Yanik J. 2015. Characterization of products from hydrothermal carbonization of orange pomace including anaerobic digestibility of process liquor. *Bioresource Technology* 196: 35-42.

[2] Benavente V., Calabuig E. and Fullana A., 2015. Upgrading of moist agro-industrial wastes by hydrothermal carbonization. *Journal of Analytical and Applied Pyrolysis* 113: 89-98.

[3] Funke A. and F. Ziegler. 2010. Hydrothermal carbonization of biomass: A summary and

discussion of chemical mechanisms for process engineering. *Biofuels, Bioproduct and Biorefining* 4: 160-177.

[4] Kambo H.S. and A. Dutta. 2015. A comparative review of biochar and hydrochar in terms of production, physico-chemical properties and applications. *Renewable and Sustainable Energy Reviews* 45: 359-378.

[5] Jamari S.S. and J.R. Howse. 2012. The effect of the hydrothermal carbonization process on palm oil empty fruit bunch. *Biomass and Bioenergy* 47: 82-90.

[6] Xiao L.-P., Shi Z.-J., Xu F., and Sun R.-C. 2012. Hydrothermal carbonization of lignocellulosic biomass. *Bioresource Technology* 118: 619-623.

[7] Zhu Z., Liu Z., Zhang Y., Li B., Lu H., Duan N., Si B., Shen R., and Lu J., 2016. Recovery of reducing sugars and volatile fatty acids from cornstalk at different hydrothermal treatment severity. *Bioresource Technology* 199: 220-227.

[8] Kongpanya J., Hussaro K. and Teekasap S., 2014. Influence of reaction temperature and reaction time on product from hydrothermal treatment of biomass residue. *American Journal of Environmental Sciences* 10(4): 324-335.

[9] Guo S., Dong X., Wu T., Shi F., and Zhu C., 2015. Characteristic evolution of hydrochar from hydrothermal carbonization of corn stalk. *Journal of Analytical and Applied Pyrolysis* 116: 1-9.

[10] Álvarez-Murillo A., Román S., Ledesma B., and Sabio E., 2015. Study of variables in energy densification of olive stone by hydrothermal carbonization. *Journal of Analytical and Applied Pyrolysis* 113: 307-314.

[11] Gao P., Zhou Y., Meng F., Zhang Y., Liu Z., Zhang W., and Xue G., 2016. Preparation and characterization of hydrochar from waste eucalyptus bark by hydrothermal carbonization. *Energy* 97: 238-245.

[12] Tekin K., Akalin M.K. and Karagöz S., 2016. The effects of water tolerant Lewis acids on the hydrothermal liquefaction of lignocellulosic biomass. *Journal of the Energy Institute* 89(4): 627-635.

[13] Erlach B., Harder B. and Tsatsaronis G., 2012. Combined hydrothermal carbonization and gasification of biomass with carbon capture. *Energy* 45(1): 329-338.

[14] Heilmann S.M., Davis H.T., Jader L.R., Lefebvre P.A., Sadowsky M.J., Schendel F.J., von Keitz M.G., Valentas K.J., 2010. Hydrothermal carbonization of microalgae. *Biomass and Bioenergy* 34(6): 875-882.

[15] Román S., Nabais J.M.V., Laginhas C., Ledesma B., and González J.F., 2012. Hydrothermal carbonization as an effective way of densifying the energy content of biomass. *Fuel Processing Technology* 103: 78-83.

[16] Centre for Agricultural Information. 2015. *Agricultural production data.* Retrieved on 30 April 2016 from the World Wide Web: http://www.oae.go.th/ewt_news.php?nid=13577.

[17] Nizamuddin S., Mubarak N.M., Tiripathi M., Jayakumar N.S., Sahu J.N., and Ganesan P., 2016. Chemical, dielectric and structural characterization of optimized hydrochar produced from hydrothermal carbonization of palm shell. *Fuel* 163: 88-97.

[18] Yuliansyah A.T., Hirajima T., Kumagai S., and Sasaki K., 2010. Production of solid biofuel from agricultural wastes of the palm oil industry by hydrothermal treatment. *Waste and Biomass Valorization* 1(4): 395-405.

[19] Department of Alternative Energy Development and Efficiency. 2013. *Biomass potential in Thailand.* Retrieved on 30 April 2016 from the World Wide Web: http://biomass.dede.go.th/biomass_web/index.html.

[20] Sluiter A., Hames B., Ruiz R., Scarlata C., Sluiter J. and Templeton D. 2005. *Determination of ash in biomass (NREL/TP-510-42622).* The US national renewable energy laboratory technical report.

[21] ASTM. 2010. *Standard Test Methods for Proximate Analysis of Coal and Coke by Macro Thermogravimetric Analysis.* Method D7582-10. ASTM International, Pennsylvania. USA.

[22] Channiwala S.A. and P.P. Parikh. 2002. A unified correlation for estimating HHV of solid, liquid and gaseous fuels. *Fuel* 81(8): 1051-1063.

[23] Zakaria M.R., Hirata S., and Hassan M.A., 2015. Hydrothermal pretreatment enhanced enzymatic hydrolysis and glucose production from oil palm biomass. *Bioresource Technology* 176: 142-148.

[24] Rather M.A., Khan N.S., and Gupta R., 2017. Hydrothermal carbonization of macrophyte Potamogeton lucens for solid biofuel production. *Engineering Science and Technology, an International Journal* 20(1): 168-174.

[25] Singh R., Balagurumurthy B., Prakash A., and Bhaskar T., 2015. Catalytic hydrothermal liquefaction of water hyacinth. *Bioresource Technology* 178: 157-165.

[26] Anastasakis K. and A.B. Ross. 2011. Hydrothermal liquefaction of the brown macro-alga Laminaria Saccharina: Effect of reaction conditions on product distribution and composition. *Bioresource Technology* 102(7): 4876-4883.

[27] Petrović J., Perišić N., Maksimović J.D., Maksimović V., Kragović M., Stojanović M., Laušević M., and Mihajlović M., 2016. Hydrothermal conversion of grape pomace: Detailed characterization of obtained hydrochar and liquid phase. *Journal of Analytical and Applied Pyrolysis* 118: 267-277.

[28] Reza M.T., Rottler E., Herklotz L., and Wirth B. 2015. Hydrothermal carbonization (HTC) of wheat straw: Influence of feedwater pH prepared by acetic acid and potassium hydroxide. *Bioresource Technology* 182: 336-344.

[29] Reza M.T., Wirth B., Lüder U., and Werner M., 2014. Behavior of selected hydrolyzed and dehydrated products during hydrothermal carbonization of biomass. *Bioresource Technology* 169: 352-361.

[30] Liu Z., Quek A., Kent Hoekman S., Srinivasan M.P., and Balasubramanian R., 2012. Thermogravimetric investigation of hydrochar-lignite co-combustion. *Bioresource Technology* 123: 646-652.

[31] Beychok M. 2012. *Coal.* Retrieved on 30 April 2016 from the World Wide Web: http://www.eoearth.org/view/article/151276.

[32] Lu X., Pellechia P.J., Flora J.R.V., and Berge N.D., 2013. Influence of reaction time and temperature on product formation and characteristics associated with the hydrothermal carbonization of cellulose. *Bioresource Technology* 138: 180-190.

[33] Garcia-Maraver A., Salvachúa D., Martínez M.J., Diaz L.F., and Zamorano M., 2013. Analysis of the relation between the cellulose, hemicellulose and lignin content and the thermal behavior of residual biomass from olive trees. *Waste Management* 33(11): 2245-2249.

[34] Zhang J., Chen T., Wu J., and Wu J., 2014. Multi-Gaussian-DAEM-reaction model for thermal decompositions of cellulose, hemicellulose and lignin: Comparison of N_2 and CO_2 atmosphere. *Bioresource Technology* 166: 87-95.

[35] Kim D., Lee K., and Park K.Y., 2014. Hydrothermal carbonization of anaerobically digested sludge for solid fuel production and energy recovery. *Fuel* 130: 120-125.

[36] Kong L., Miao P. and Qin J., 2013. Characteristics and pyrolysis dynamic behaviors of hydrothermally treated micro crystalline cellulose. *Journal of Analytical and Applied Pyrolysis* 100: 67-74.

[37] Hisaya T., Pilasinee L., Tsuyoshi H., Keiko S., Hajime M., and Satoshi K., 2014. Recovery of Furfural Produced by Hydrothermal Treatment with Biomass Charcoal. *International Journal of Environment* 4(1): 11-17.

[38] Hu L., Zhao G., Hao W., Tang X., Sun Y., Lin L., and Liu S., 2012. Catalytic conversion of biomass-derived carbohydrates into fuels and chemicals via furanic aldehydes. *RSC Advances* 2(30): 11184-11206.

[39] Ju M., Zeng C., Wang C., and Zhang L., 2014. Preparation of ultrafine carbon spheres by controlled polymerization of furfuryl alcohol in microdroplets. *Industrial and Engineering Chemistry Research* 53(8): 3084-3090.

[40] Guo Z., Theng D.S., Tang K.Y., Zhang L., Huang L., Borgna A. and Wang C., 2016. Dehydration of lactic acid to acrylic acid over lanthanum phosphate catalysts: the role of Lewis acid sites. *Physical Chemistry Chemical Physics* 18(34): 23746-23754.

[41] Antal Jr., M.J., Mok W.S.L., and Richards G.N., 1990. Mechanism of formation of 5-(hydroxymethyl)-2-furaldehyde from d-fructose and sucrose. *Carbohydrate Research* 199(1): 91-109.

[42] Titirici M.-M., Funke A., and Kruse A., 2015. Chapter 12 - Hydrothermal Carbonization of Biomass. In A. Pandey, T. Bhaskar, M. Stöcker, K. Rajeev eds. *Recent Advances in Thermo-Chemical Conversion of Biomass*: Elsevier. Boston, USA, 325-352.

[43] Mukherjee A., Dumont M.-J., and Raghavan V., 2015. Review: Sustainable production of hydroxymethylfurfural and levulinic acid: Challenges and opportunities. *Biomass and Bioenergy* 72: 143-183.

[44] Jin F., Yun J., Li G., Kishita A., Tohji K., and Enomoto H., 2008. Hydrothermal conversion of carbohydrate biomass into formic acid at mild temperatures. *Green Chemistry* 10(6): 612-615.

[45] Amass W., Amass A., and Tighe B., 1998. A review of biodegradable polymers: uses, current developments in the synthesis and characterization of biodegradable polyesters, blends of biodegradable polymers and recent advances in biodegradation studies. *Polymer International* 47(2): 89–144.

[46] Poerschmann J., Weiner B., Wedwitschka H., Zehnsdorf A., Koehler R., and Kopinke F.D., 2015. Characterization of biochars and dissolved organic matter phases obtained upon hydrothermal carbonization of Elodea nuttallii. *Bioresource Technology* 189: 145-153.

[47] Zhang A. and S.-T. Yang. 2009. Propionic acid production from glycerol by metabolically engineered Propionibacterium acidipropionici. *Process Biochemistry* 44(12): 1346-1351.